Collisions of DCl with a Solution Covered with Hydrophobic and Hydrophilic Ions: Tetrahexylammonium Bromide in Glycerol†

Susan M. Brastad, Daniel R. Albert, Mingwei Huang, and Gilbert M. Nathanson*

Department of Chemistry, University of Wisconsin−Madison, 1101 University Avenue, Madison, Wisconsin 53706-1322

Received: January 9, 2009; Revised Manuscript Received: March 14, 2009

Gas−liquid scattering experiments are used to investigate interfacial interactions of gaseous DCl with liquid glycerol containing 0.03 M tetrahexylammonium bromide (THABr), an ionic surfactant composed of hydrophobic THA^+ and hydrophilic Br^- ions. Surface tension and argon scattering measurements indicate that the surface of this solution is dominated by the hexyl chains of the THA^+ ion. The hydrocarbon character of the surface is further explored by comparing Ar and DCl scattering from the THABr solution and liquid squalane. We find that the addition of THABr to glycerol alters the reactivity of DCl in two ways: DCl molecules that land on the surface are more likely to desorb when THA^+ and Br^- are present and are less likely to dissolve, but they are also more likely to undergo rapid, interfacial DCl → HCl exchange. Similar trends are observed when THA^+ ions are replaced by Na^+ ions in a 2.7 M NaBr solution, even though THA^+ interacts weakly with glycerol OH groups and Na^+ binds strongly to them. These observations suggest that the THA^+ hexyl chains do not physically block DCl entry and that interfacial cation−OH bonding is not essential for promoting rapid D → H exchange when Br^-−OH bonding also occurs. The use of THABr confirms that ions in the top few monolayers, and not those deeper in solution, control DCl entry and rapid D → H exchange.

Introduction

Tetraalkylammonium halide salts have long been studied for their hydrophobic and surfactant properties.[1−5] In water, these salts decrease the surface tension when the alkyl chain is composed of two or more carbon atoms.[5] This reduction implies an excess of ions in the interfacial region and makes these organic salts true ionic surfactants. Surface-sensitive techniques, such as ion scattering[6,7] and photoelectron spectroscopy,[8−13] along with recent computer simulations,[11,12,14−17] provide a microscopic view of the tetraalkylammonium cation and halide anion at the surfaces of water and formamide. They reveal that tetrabutylammonium resides at the outermost surface layer, intermixed with Br^- or I^-, but that the smaller and less polarizable Br^- is less confined to the surface.[6,7,12,18] On average, three of the tetrahedrally oriented butyl chains point primarily along the surface while the fourth points inward toward the liquid.[10,11,13,17] Computer simulations indicate that the alkyl groups coat much of the surface, with gaps filled by halide ions and by solvent molecules, as shown in Figure 1 for tetrabutylammonium iodide in water.[11] This snapshot demonstrates vividly that surface OH groups point toward iodide but form a hydrogen-bonding network around the butyl chains.

How might the presence of this hydrocarbon "shell" alter reactions at gas−liquid interfaces? We have previously explored collisions of DCl molecules with liquid glycerol [$HOCH_2CH(OH)CH_2OH$], a low-vapor pressure (10^{-4} Torr) and viscous (1400 cP) fluid that dissolves acids, bases, and salts with water-like solubilities.[19−21] As shown in Figure 2a, DCl molecules may scatter impulsively from the surface of glycerol (pathway a) in one or a few collisions or fully dissipate their kinetic energy and become momentarily trapped (b), in part by forming hydrogen bonds with interfacial glycerol OH groups.[22] At thermal collision energies approaching $2RT_{liq} \approx 5$ kJ mol^{-1}, nearly all impinging DCl molecules are trapped momentarily on the surface. These thermalized molecules either desorb immediately as intact DCl (c), undergo near-interfacial D → H exchange and desorb as HCl (d), or become solvated as Cl^- and D^+/H^+ in the bulk (e) and then slowly evaporate (f). The addition of KI, NaI, NaBr, LiI, and CaI_2 at molar concentrations to glycerol significantly enhances nonreactive DCl desorption *and* near-interfacial D → H exchange at the expense of bulk entry.[23−25] NaI, NaBr, and LiI cause similar changes, whereas KI and CaI_2 are less and more effective, respectively, than the other salts. We attributed these ion-catalyzed processes to the

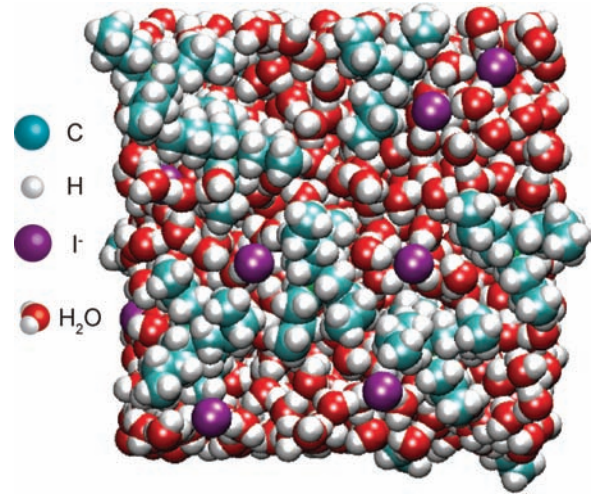

Figure 1. Snapshot of a molecular dynamics simulation showing a top view of the surface of a ∼1 molal solution of tetrabutylammonium iodide in water. Reprinted with permission from ref 11.

† Part of the "Robert Benny Gerber Festschrift".

* Corresponding author. E-mail: nathanson@chem.wisc.edu.

10.1021/jp900232v CCC: $40.75
Published on Web 04/14/2009

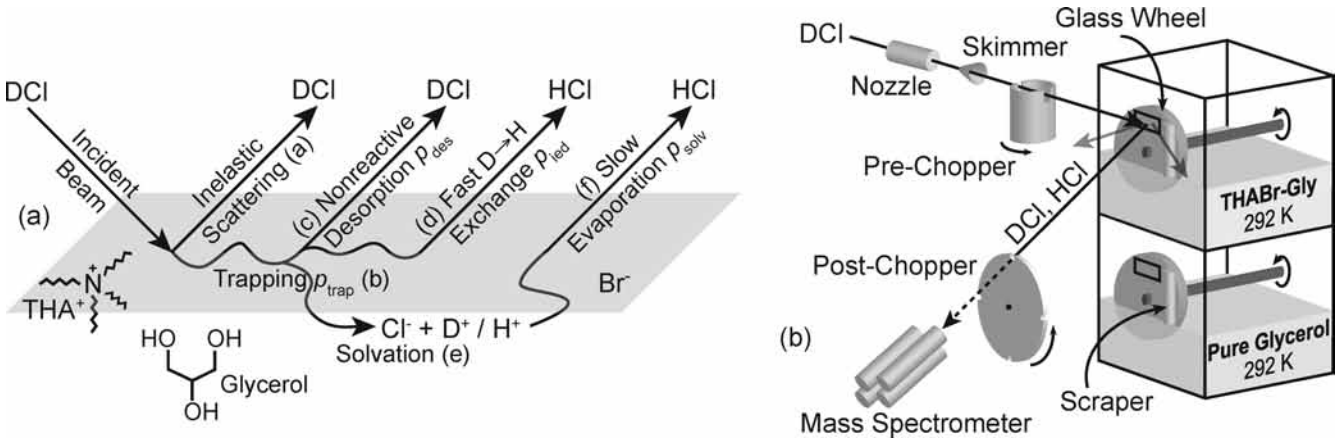

Figure 2. (a) Observed reaction pathways for collisions of DCl molecules with a 0.03 M THABr−glycerol solution. (b) Scattering apparatus.

formation of bonds between interfacial OH groups and I^-, Br^-, K^+, Na^+, and Ca^{2+} ions, which potentially modify the surface region in two distinct ways: ion−OH bonds remove sites for DCl adsorption and dissociation, enhancing nonreactive desorption, and they interrupt the hydrogen bonding network that carries H^+ away from the more slowly moving Cl^-, thereby promoting their recombination. Will these trends remain the same when the alkali cation is replaced by a hydrophobic one and when a concentrated ionic solution is replaced by a dilute surfactant solution?

Tetrahexylammonium bromide (THABr) was chosen to ensure that the carbon chain would be long enough for the ion to segregate to the surface, even when the bulk concentration is low.[5,26] We initially believed that the large and weakly coordinating THA^+ ion would enhance nonreactive DCl desorption and suppress both bulk dissolution and near-interfacial D → H exchange. As described below, this expectation is only partly correct: interfacial Br^- and THA^+ ions in a 0.03 M THABr−glycerol solution do cause more adsorbed DCl molecules to desorb before they can dissolve, but the addition of THABr also enforces more near-interfacial D → H exchange. A concentrated, 2.7 M NaBr solution with similar surface ion densities behaves in parallel ways. These common trends imply that the THA^+ ion does not block bulk solvation more efficiently than Na^+, despite its appearance as a surfactant "covering" in Figure 1.

Surface Tensions and Compositions of THABr−Glycerol and −Water Solutions. Solutions of THABr in water form two liquid phases at 298 K with concentrations of 0.02 and 9 molal THABr.[27] A similar two-phase system was observed for solutions of THABr in glycerol, in which the dilute phase is 0.05−0.07 molal THABr. The surface tensions of THABr−water and −glycerol solutions in the single phase region up to 0.02 and 0.03 molal, respectively, are shown in Figure 3 at 292 K. These measurements were made using the Wilhelmy method with a 1.0 mm diameter Pt pin. The addition of THABr to water and glycerol decreases the surface tension, σ, from 72 to 42 dyn cm^{-1} in water and 64 to 41 dyn cm^{-1} in glycerol. The dashed lines in Figure 3 represent a least-squares fit to a Langmuir adsorption isotherm. This fit is used to determine the surface excess of THABr from the Gibbs adsorption equation[15,28]

$$\Gamma_{ion} = \Gamma_{THA^+} + \Gamma_{Br^-} = \frac{-1}{kT}\left(\frac{\partial\sigma}{\partial \ln \gamma_{\pm} m}\right)_T \qquad (1)$$

where m is the THABr molality and $\gamma_{\pm}$ is the mean molal activity coefficient for THABr. The surface excess is plotted on the right-hand axis in Figure 3 with $\gamma_{\pm} = 1$. The individual

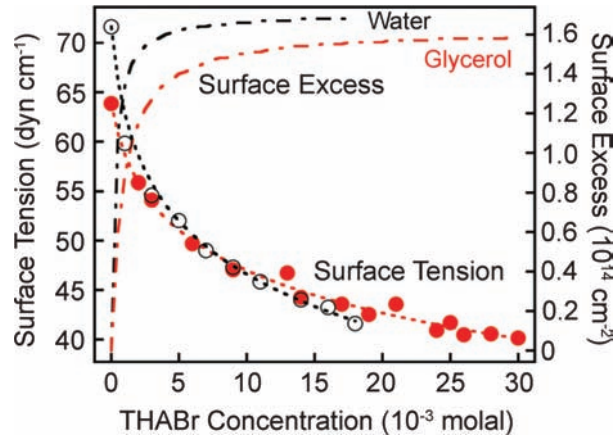

Figure 3. Surface tension measurements of THABr−water (black ○) and THABr−glycerol (red ●) solutions. The dashed lines are fits to the experimental data. The THABr surface excess in water (black) and glycerol (red), determined from the fits, is plotted on the right-hand axis.

surface excesses of THA^+ and Br^- are $\Gamma_{ion}/2$, equal to ~9 × 10^{13} cm^{-2} in water and ~8 × 10^{13} cm^{-2} in glycerol at the highest THABr concentration.[29] The curves in Figure 3 highlight the similar surface propensities of THABr in water and glycerol, providing motivation for using the snapshot in Figure 1 to visualize the behavior of tetraalkylammonium salts in glycerol.

The THA^+ and Br^- surface excesses can be interpreted further if the positions of the ions are known at the atomic scale. Ion scattering and computer simulations of tetrabutylammonium and tetrabutylphosphonium cations suggest that THA^+ ions should be located predominantly in the top layer of the solution,[6,7,10−12,14,17,30] a feature corroborated by the argon scattering experiments below. The ion scattering studies also indicate that, in formamide, the Br^- counterion is located mostly at the surface in a valley-like structure,[7] whereas simulations of tetrabutylammonium in a mixed I^- and Br^- aqueous solution predict that Br^- lies at or near the surface but is distributed slightly more broadly than I^- into the bulk.[12] On the basis of these studies, we estimate the surface composition by assuming that the excess THA^+ and Br^- ions are both confined to the top layer.[31] Using $\Gamma_{THA^+} = \Gamma_{Br^-} = 8 \times 10^{13}$ cm^{-2} and cross-sectional areas of ~70 $Å^2$ for THA^+, ~10 $Å^2$ for Br^-, and ~25 $Å^2$ for glycerol,[32] the fraction of surface area occupied by each species is ~55% THA^+, ~8% Br^-, and ~37% glycerol for 0.025 molal (0.031 M) THABr. These fractions correspond to only ~1 glycerol molecule for every Br^- and THA^+ ion within the top layer. This ratio rises to ~2 glycerol per THA^+ ion in the unlikely event that all Br^-

ions are excluded from the top layer. In comparison, the same 0.03 M THABr−glycerol solution corresponds to ∼220 glycerol molecules per ion in the bulk.

The surface tensions of 0−3 molal NaBr−glycerol solutions were found to rise linearly with concentration with a slope of ∼1.5 dyn cm^{-1} $molal^{-1}$. This value and the Gibbs equation yield a total ion surface deficit of -3×10^{13} cm^{-2} using activity coefficients for NaI in glycerol.[33] Assuming that this deficit is confined to the outermost monolayer,[25] the Br^- and Na^+ concentrations in this layer for a 2.7 M NaBr−glycerol solution are $\sim 7 \times 10^{13}$ cm^{-2}, a value that will rise if the deficit is spread over several layers. This minimum surface concentration lies just below the $\sim 8 \times 10^{13}$ cm^{-2} values for THA^+ and Br^- in the 0.03 M THABr solution. In water, Br^- lies above Na^+ near the surface, forming a diffuse, overlapping double layer.[15] The surface tension, ion scattering, and molecular dynamics studies together suggest that Br^- ions are likely to be found in or near the top layer in roughly equal amounts in the THABr− and NaBr−glycerol solutions, situated alongside or just below THA^+ ions and mostly above Na^+ ions.

Gas−Liquid Scattering Experiments. The 0.03 M THABr−glycerol solution is made by adding THABr (Fluka, 99.0+%) to glycerol (Aldrich, 99.5+%) that has been degassed and dewatered.[24] Aliquots (50 mL) of the THABr solution and pure glycerol are then added to the stacked liquid reservoirs shown in Figure 2b. Each reservoir contains a vertical glass wheel partially submerged in the liquid. As the wheel rotates, it picks up a film of the viscous liquid. The film passes by a Teflon bar, which scrapes it to a uniform thickness of 0.3 mm. It is then exposed to incident beams of Ar or DCl at $\theta_{inc} = 45°$. The exposure time, t_{exp}, is determined by the speed of the rotating glass wheel and the 4.6-mm-wide beam spot. The wheel speed is 0.33 Hz ($t_{exp} = 0.12$ s) for the glycerol solutions, but is increased to 0.58 Hz ($t_{exp} = 0.07$ s) for squalane because of its lower viscosity. The incident Ar and DCl beams have peak translational energies of $E_{inc} = 90$ kJ mol^{-1} ($37RT_{liq}$), characterized by narrow energy distributions, $E_{inc}/\Delta E$, of ≥ 5/1 (in comparison with ∼1/2 for a Maxwellian beam).[20]

Molecules leaving the liquid (Ar, DCl, and HCl) are detected by a differentially pumped mass spectrometer at an exit angle of $\theta_{fin} = 45°$.[23] We use a spinning postchopper wheel to monitor the velocities of molecules leaving the liquid and a spinning prechopper wheel to monitor the residence times of the gas species in solution, as depicted in Figure 2b. In the postchopper configuration, the incident DCl or Ar beam strikes the liquid continuously. The exiting molecules are then chopped into 40 μs pulses that travel 19.5 cm to the mass spectrometer over times that depend on their velocities. These arrival times are recorded as time-of-flight (TOF) spectra. In the prechopper configuration, the incident beam is divided into 50 μs pulses striking the liquid in 2 ms intervals. The final arrival time at the mass spectrometer is the sum of the gas-phase flight times of the molecule before and after interaction with the liquid and the residence time of the solute (DCl, HCl, $Cl^-/H^+/D^+$) in solution. Previous studies demonstrate that this prechopper technique can be used to measure average residence times from 10^{-6} to 10^{-2} s.[21,23]

Results and Analysis

Argon Atom Scattering. High-energy argon atom scattering can be used to detect hydrocarbon species at the surface of glycerol because of the change in mass and roughness that occur upon segregation of the alkyl chains.[34] Figure 4 shows postchopper TOF spectra of 90 kJ mol^{-1} Ar atoms colliding with pure glycerol, 0.03 M THABr−glycerol, and squalane at $\theta_{inc} = \theta_{fin} = 45°$. Each spectrum is composed of two components: Ar atoms that inelastically scatter (IS) from the surface and those that thermally desorb (TD). The broad component at later arrival times (low exit velocities) is fit well by a Maxwell−Boltzmann distribution at the temperature of the liquid. These Ar atoms fully dissipate their incident energy and become thermalized on the surface, desorbing with an average energy of $2RT_{liq} \approx 5$ kJ mol^{-1}. Ar atoms that scatter inelastically from the surface after one or a few bounces retain a significant fraction of their incident energy and arrive at the mass spectrometer at early times (higher exit velocities).

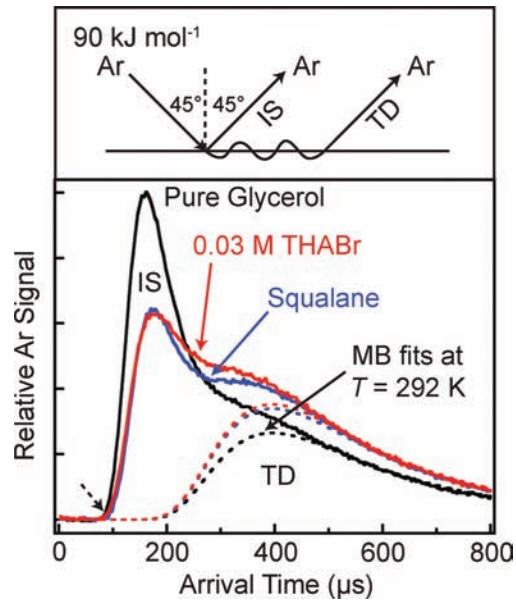

Figure 4. Postchopper TOF spectra of Ar atoms following collisions with pure glycerol (black), 0.03 M THABr−glycerol (red), and squalane (blue). The dashed lines are Maxwell−Boltzmann (MB) fits at 292 K to the thermal desorption (TD) components. "IS" refers to inelastic scattering. The dashed arrow indicates the peak arrival time of elastically scattered Ar atoms.

The addition of THABr to glycerol significantly alters collisions of Ar atoms with the surface, as shown in Figure 4. Fewer Ar atoms scatter directly from the surfactant-coated surface, and more undergo thermal desorption. These changes arise from the presence of hexyl chains at the surface, which deflect the Ar atoms over a wide range of angles and create a rougher surface that causes more Ar atoms to undergo multiple collisions and dissipate their energy. We have also observed similar changes in Ar scattering when aqueous sulfuric acid is coated with a monolayer of neutral and protonated hexanol molecules.[35]

The hydrocarbon-like nature of the THABr−glycerol surface can be further gauged by comparing this mixture to liquid squalane ($C_{30}H_{62}$; 2,6,10,15,19,23-hexamethyltetracosane).[36] Ar scattering from squalane and THABr−glycerol in Figure 4 generate nearly identical patterns, implying that the THABr−glycerol surface is dominated by alkyl chains. These comparisons, in conjunction with the surface tension measurements, indicate that THA^+ ions must substantially cover the surface of the solution.

DCl → DCl Scattering. We first explore collisions of DCl with glycerol that lead to inelastic scattering (channel a in Figure 2a) or nonreactive desorption (channel c). Figure 5a shows postchopper spectra of 90 kJ mol^{-1} DCl molecules recoiling from the surfaces of pure glycerol and squalane. Each spectrum

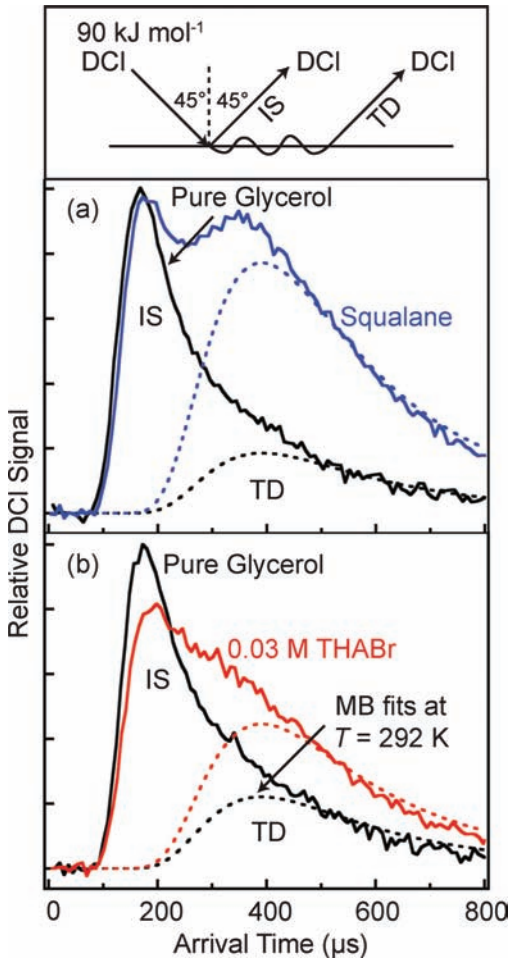

Figure 5. Postchopper TOF spectra of HCl molecules following collisions of DCl with pure glycerol and (a) squalane and (b) 0.03 M THABr−glycerol. The dashed lines are Maxwell−Boltzmann (MB) fits at 292 K to the thermal desorption (TD) components. "IS" refers to inelastic scattering.

is composed of DCl molecules that scatter directly from the surface or thermalize and then desorb, following the pattern in Ar scattering. The much smaller DCl desorption signal from glycerol (labeled as "TD") is a signature of the extensive loss of DCl into the protic liquid, as described below. In contrast, nearly all DCl molecules that thermalize on the surface of squalane desorb back into the gas phase.[37]

Figure 5b shows that DCl molecules also desorb more often from the THABr solution than from pure glycerol, although the change is not as large as for squalane. This increase in thermal desorption implies that fewer DCl molecules react with the THABr solution than with pure glycerol. We postulate later that this reduced reactivity arises not only from hexyl chains at the surface but also from OH−Br^- bonds that remove sites for DCl adsorption and dissociation.

The inelastic scattering (IS) components in Figure 5 reveal surprising trends. Panel a shows that 90 kJ mol^{-1} DCl molecules scatter with the same intensity from pure glycerol and squalane at $\theta_{inc} = \theta_{fin} = 45°$. We initially expected the IS channel to be smaller from squalane than from glycerol, in analogy with Ar atom scattering in Figure 4. The weaker DCl signal from glycerol may arise from strong attractions between DCl and surface OH groups during the picosecond time in which DCl bounces along the surface. The nearly equal IS signals may also be an accidental overlap of the different DCl angular distributions from squalane and glycerol. However, measurements at

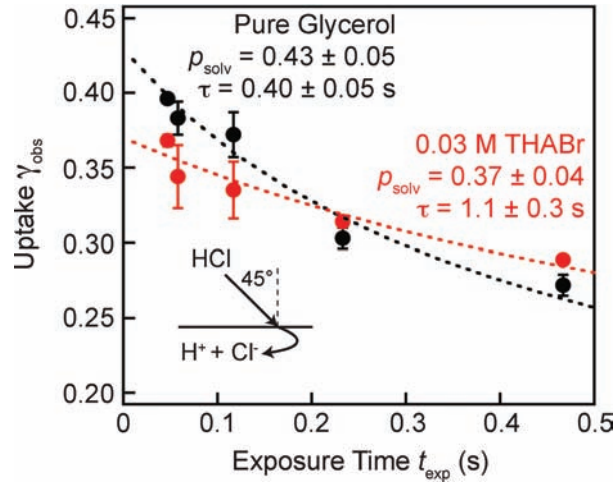

Figure 6. HCl uptake, $\gamma_{obs}(t_{exp})$, vs exposure time, t_{exp}, for pure glycerol (black) and 0.03 M THABr−glycerol (red). The fits to the data yield the entry probability, p_{solv}, and the bulk-phase residence time, τ, of HCl in solution. The error bars for the data points represent the difference in two measurements, producing error bars for τ and p_{solv} that represent the uncertainty in fitting the data.

incident angles of $\theta_{inc} = 30°$ and 54° ($\theta_{fin} = 60°$ and 36°) also produce equal IS intensities, suggesting that the angular distributions are similar in the forward direction. In comparison, panel b shows that the inelastic scattering of DCl from 0.03 M THABr is weaker than from pure glycerol, mimicking the changes in Ar scattering. Both surfaces contain OH groups in this case, and the primary distinction may be the enhanced roughness imposed by the hexyl chains, which scatter both DCl and Ar over a wider angular range.

DCl Uptake Measurements. As depicted in Figure 2a, DCl molecules may also enter glycerol and dissociate into Cl^- and D^+/H^+ (channel e). We use beam reflectivity measurements to monitor the fraction of DCl molecules that enter the liquid and the time they remain solvated as ions.[20] To improve signal stability in these long experiments, the DCl beam is replaced by HCl. The uptake is measured by directing ~100 kJ mol^{-1} HCl molecules at the liquid in the reservoir, which is exposed to the beam for a time t_{exp}.[38] The HCl partial pressure is monitored in the chamber at $m/z = 36$ when the beam is blocked by a Teflon flag, P_{flag}, incident on the liquid, P_{liq}, and blocked from entering the chamber, P_{bkg}. The observed uptake $\gamma_{obs}(t_{exp})$ is then equal to $(P_{flag} - P_{liq})/(P_{flag} - P_{bkg})$. This fraction is equal to 1 if all of the HCl enters and remains in the solution over the time t_{exp} and 0 if no HCl enters the solution or if the flux of HCl molecules leaving the liquid equals the flux into the liquid.

Entry Probabilities. The observed uptake measurements for HCl into pure glycerol and 0.03 M THABr−glycerol are shown in Figure 6. For both liquids, the net uptake, γ_{obs}, decreases with increasing exposure time. This decrease in γ_{obs} occurs because H^+ and Cl^- ions that build up in solution slowly recombine and desorb, thereby decreasing the net flux of HCl molecules entering the solution. The dotted lines in the figure are fits to the data calculated from liquid phase diffusion and flux balancing at the gas−liquid boundary.[23] The fits depend on two quantities: the absolute entry probability, p_{solv}, and the characteristic residence time, τ, of H^+ and Cl^- in solution. The probability p_{solv} is equal to the fraction of HCl molecules that enter the solution at $t_{exp} = 0$ s when there is no H^+ or Cl^- present in the solution. As shown in Figure 6, the value for $p_{solv} = \gamma_{obs}(t_{exp} = 0)$ is 0.43 ± 0.05 for pure glycerol, indicating that 43% of HCl molecules enter pure glycerol at $E_{inc} \approx 100$ kJ

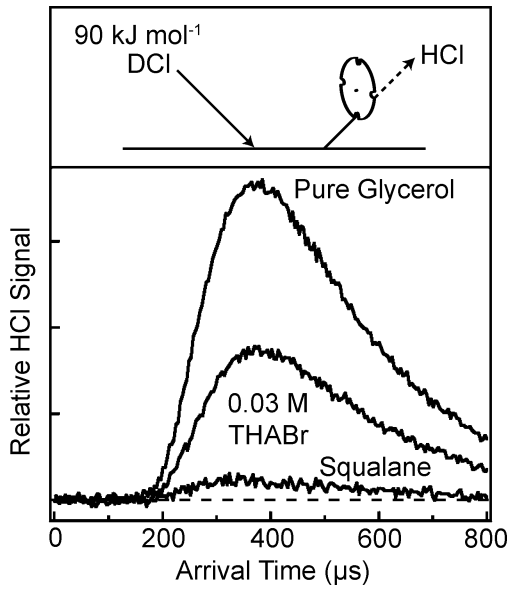

Figure 7. Postchopper TOF spectra of HCl molecules following collisions of DCl with pure glycerol, 0.03 M THABr−glycerol, and squalane. The dashed line represents zero signal.

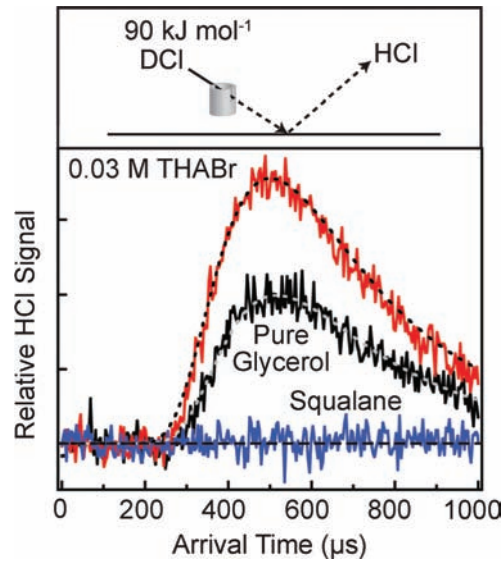

Figure 8. Prechopper TOF spectra of HCl following collisions of DCl with pure glycerol (black), 0.03 M THABr−glycerol (red), and squalane (blue). The dashed lines are fits to a bulk phase residence time τ of 10^{-6} s.

mol^{-1} and $\theta_{inc} = 45°$. This fraction drops to 0.37 ± 0.04 when THABr is added to glycerol, indicating that the entry of HCl is impeded by the addition of the surfactant.

Bulk-Phase Solvation Times. The shape of each curve in Figure 6 is determined by a characteristic residence time, τ, of Cl^- and H^+ in solution (described in the Appendix), which is equal to the time for the desorbing HCl flux to reach ~49% of the HCl flux that enters the solution. Figure 6 shows that the observed uptake drops from 0.43 at $t_{exp} = 0$ s to 0.26 at $t_{exp} = 0.5$ s for pure glycerol, and from 0.37 to 0.28 for 0.03 M THABr−glycerol over the same exposure time. The shallower curve for THABr−glycerol yields $\tau = 1.1 \pm 0.3$ s, in comparison with $\tau = 0.40 \pm 0.05$ s for pure glycerol. As shown in the Appendix, this nearly 3-fold increase in τ for the THABr−glycerol solution arises from the decrease in activity coefficients of H^+ and Cl^- upon adding THABr to glycerol and from the lower HCl entry probability into the THABr solution.

HCl Evaporation. The observed dependence of γ_{obs} on t_{exp} implies that the net uptake changes with time because of HCl evaporation following Cl^- and H^+ recombination. This evaporation is monitored directly in Figure 7, which compares postchopper spectra of HCl desorbing from pure glycerol and 0.03 M THABr−glycerol following collisions of 90 kJ mol^{-1} DCl molecules at $t_{exp} = 0.12$ s. As expected from the uptake data in Figure 6, the HCl signal from 0.03 M THABr−glycerol is weaker than from pure glycerol due to the longer residence time of H^+ and Cl^- in the THABr solution. Also shown in Figure 7 is the HCl desorption signal from squalane following collisions of DCl, which was not anticipated.[39] We attribute this weak HCl signal to DCl molecules that react with an OH-containing impurity in squalane, possibly one that is observed to evaporate with a mass of ~240 amu. By comparing this HCl signal to that from pure glycerol, we estimate that it corresponds to only ~0.5% conversion of the impinging DCl beam into HCl.

Previous studies of DCl collisions with a 2.7 M NaBr−glycerol solution reveal that HBr desorbs from solution following exposure to DCl.[24] These HBr molecules are generated from recombination of Br^- with D → H-exchanged H^+. We were unable to observe HBr desorption from the 0.03 M THABr−glycerol solution, most likely because Br^- is 90 times more dilute than in the NaBr solution and because of the much greater solubility of HBr than of HCl. The absence of HBr implies that DCl → HBr conversion does not occur immediately in the interfacial region, where the concentration of Br^- ions in the THABr and NaBr solutions are similar.

Rapid, Near-Interfacial D → H Exchange. Submicrosecond production of HCl following collisions of DCl (channel d in Figure 2a) can be monitored by directing 50 μs pulses of DCl at the surface and recording the HCl arrival time, which is the sum of the gas phase flight times and the residence time of Cl-containing species (HCl, DCl, Cl^-) in solution.[21] When the residence time, τ, is 0, the thermal distribution of HCl desorption velocities determines the distribution of HCl arrival times at the mass spectrometer. Average residence times greater than 10^{-6} s measurably broaden the arrival time distribution because a small fraction of the molecules dissolve deeply and desorb over a range of times that shift the desorption spectrum toward longer arrival times. When τ exceeds 10^{-2} s, the molecules desorb over such a broad range of times that they merge with the background and are not detectable.

Figure 8 compares prechopper spectra of HCl following collisions of DCl with pure glycerol, THABr−glycerol, and squalane. The HCl desorption signal from squalane was not detectable, implying that the residence times of HCl monitored in the postchopper spectrum in Figure 7 must exceed 10^{-2} s. This long time corresponds to a diffusion depth of $(D\tau/2)^{1/2} >$ 5000 Å for $\tau > 10^{-2}$ s and $D \approx 5 \times 10^{-7}$ cm^2 s^{-1} for HCl in squalane.[40] The absence of rapid HCl desorption from squalane confirms that Cl^- and H^+ ions generated by impinging DCl molecules must remain dissolved for long times before recombining, most likely because of their low concentration in solution (generated by a low concentration of protic impurities).

In contrast, HCl desorption is readily observed following collisions of DCl with pure glycerol and the THABr solution. As shown in Figure 8, the prechopper signal is well-fit with a characteristic residence time τ of 10^{-6} s,[21] indicating that a fraction of the DCl molecules undergo rapid D → H exchange within a shallow depth of $(D\tau/2)^{1/2} \approx 10$ Å for $D \approx 4 \times 10^{-8}$ cm^2 s^{-1} in glycerol.[20] Figure 8 further reveals that more D → H exchanged HCl molecules desorb immediately from the

surfactant-coated glycerol solution than from pure glycerol. This comparison implies that the addition of THABr does not inhibit near-interfacial proton exchange but instead enhances it.

Reaction Probabilities. The branching fractions for the pathways in Figure 2a are determined from the entry probabilities, p_{solv}, listed in Figure 6 and from the intensities of the TOF spectra in Figures 5b and 8. In this analysis, we assume only that the angular distributions of the thermally desorbing DCl and HCl molecules are the same for pure glycerol and 0.03 M THABr−glycerol (and are likely cosine). This equality implies that the ratios of the TD fluxes at $\theta_{inc} = 45°$ are equal to the ratios of the angle-integrated fluxes. The probabilities for nonreactive DCl trapping and desorption, $p_{trap\text{-}desorb}$, and near-interfacial D → H exchange, p_{ied}, are then given by

$$p_{trap\text{-}desorb(THABr)} = \left(\frac{I^{DCl\ TD}_{post(THABr)}}{I^{DCl\ TD}_{post(pure)}}\right) p_{trap\text{-}desorb(pure)} \quad (2)$$

$$p_{ied(THABr)} = \left(\frac{I^{HCl\ TD}_{pre(THABr)}}{I^{HCl\ TD}_{pre(pure)}}\right) p_{ied(pure)} \quad (3)$$

where I is the desorption flux integrated over the arrival times in the pre- and postchopper spectra.[24] The trapping probability, p_{trap}, of DCl on the surface of the liquid is then equal to $p_{trap\text{-}desorb} + p_{ied} + p_{solv}$. This value has previously been determined to be 0.49 ± 0.01 for pure glycerol from 23 measurements at $E_{inc} = 90$ kJ mol^{-1} and $\theta_{inc} = 45°$. For 0.03 M THABr and 2.7 M NaBr, we find that $p_{trap} = 0.49 \pm 0.04$ and 0.45 ± 0.04, respectively.

The branching fractions $p_{trap\text{-}desorb}/p_{trap}$, p_{ied}/p_{trap}, and p_{solv}/p_{trap} for pure glycerol and 0.03 M THABr−glycerol are shown in Figure 9. We report these fractions instead of the individual probabilities because they are more reproducible, and as the incident energy approaches thermal conditions of $2RT_{liq} \approx 5$ kJ mol^{-1}, p_{trap} approaches 1 and the branching fractions become equal to the individual probabilities at thermal collision energies.[21] Figure 9 shows that a thermalized DCl molecule is twice as likely to desorb from the THABr solution as it is from pure glycerol and is nearly twice as likely to undergo rapid, near-interfacial D → H exchange and desorb as HCl. The enhancements in these two reaction pathways correspond to a decrease in the fraction of thermalized DCl molecules that pass through the interfacial region and enter the solution as intact DCl or as D^+/H^+ and Cl^-.

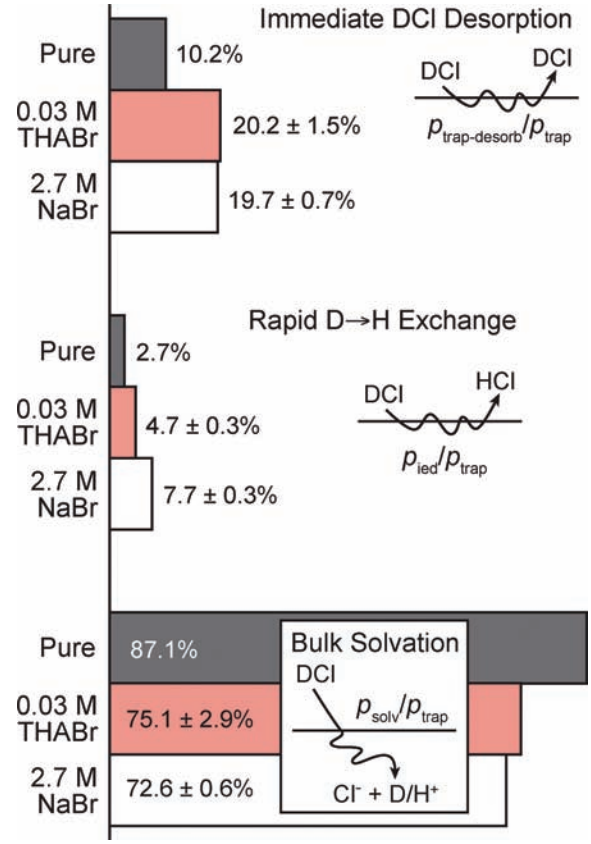

Figure 9. Branching fractions for collisions of DCl with pure glycerol, 0.03 M THABr−glycerol, and 2.7 M NaBr−glycerol. In the middle bar graph, "ied" refers to immediate D → H exchange followed by HCl desorption. The trapping probabilities, p_{trap}, are 0.49 for pure glycerol, 0.49 for 0.03 M THABr−glycerol, and 0.45 for 2.7 M NaBr−glycerol at $E_{inc} = 90$ kJ mol^{-1} and $\theta_{inc} = 45°$. The error bars for THABr−glycerol represent the difference between two measurements. Branching fractions for NaBr are adapted from ref 24.

Discussion

The behavior of a 0.03 M THABr−glycerol solution shown in Figure 9 mimics the trends previously observed for bromide and iodide salts. Solutions of NaI, KI, LiI, NaBr, and CaI_2 also enhance nonreactive DCl desorption and rapid D → H exchange at the expense of bulk solvation.[24,25] For comparison, Figure 9 lists the reaction probabilities for a 2.7 M NaBr−glycerol solution, which are similar to the THABr solution for nonreactive DCl desorption and bulk entry but nearly twice as large for rapid D → H exchange.[41] We argue below that these trends are due to similar Br^- surface concentrations in the THABr and NaBr solutions and to the weak interference of the THA^+ cation.

Ion-Mediated Blocking of DCl Ionization. The tetrabutylammonium iodide−water surface in Figure 1 highlights two possible roles for Br^- and THA^+ in enhancing DCl desorption from glycerol: OH−Br^- bonding and THA^+ site blocking. In water, THA^+ is a hydrophobic ion that sits in a cavity about which water molecules form tightly connected H_2O-H_2O hydrogen bonds (as depicted in Figure 1 for tetrabutylammonium).[3,16,42,43] There is no evidence that water molecules reorient toward the THA^+ positive charge, most likely because this charge is dispersed among the four carbon atoms attached to the nitrogen atom[3,44] and because of the stability gained by knitting hydrogen bonds around and between the alkyl chains.[3] In aqueous alkali halide solutions, however, water molecules reorient toward the hydrophilic Br^- and Na^+ ions in the first hydration shell and bind strongly to them.[45−50] The formation of OH−ion bonds was used previously to explain enhanced DCl desorption by concentrated alkali halide−glycerol solutions.[24] In this scenario, anions (Br^-, I^-) and cations (Li^+, Na^+, and K^+) in the interfacial region bind to glycerol OH groups and reduce the number of adsorption sites for incoming DCl molecules. This prebonding suppresses DCl dissociation, which requires the formation of two hydrogen bonds to Cl and one to D in order to ionize DCl to the contact ion pair.[22,51]

The hydrophobic nature and large size of THA^+ instead raise the possibility that this ion physically blocks impinging DCl molecules from making contact with glycerol OH groups lying underneath the hexyl chains. This single CH_2 layer is likely to be porous, however, if the DCl molecules reside long enough at the surface to diffuse around the chains and bond to neighboring OH groups. Figure 9 places an upper limit on the resistance of the hexyl film and OH−Br^- bonds to gas transport: nonreactive DCl desorption increases from 10% for pure glycerol to only 20% for THABr−glycerol, which is the same change brought about by the NaBr solution at a similar surface

ion concentration. This comparison suggests that chain blocking, although visually startling in the snapshot in Figure 1, does not play a larger role than OH−Na^+ bonding in controlling the immediate desorption of thermalized DCl molecules from the surface of glycerol (assuming that Br^- ions act similarly in each solution). Both OH−Br^- bonding and hexyl chain site blocking for the THABr solution must be relatively ineffective in suppressing DCl entry and dissociation in view of the high surface density of hexyl chains and of Br^- ions, which may leave only ∼1/3 of the surface composed of glycerol molecules. The permeability of surface hexyl chains is not limited to THABr in glycerol: we have observed similar porosities for films of neutral and protonated hexanol molecules at the surface of aqueous sulfuric acid at 213 K. These films impede HCl entry and water evaporation by at most 25%, even when the hexyl chains cover the surface at densities corresponding to 68% of a close-packed, upright monolayer.[35]

Ion-Mediated Interfacial D → H Exchange. Figure 9 also shows that the THABr film enhances immediate D → H exchange, although not as effectively as the NaBr solution. The enhancements in alkali halide solutions were again rationalized by the formation of OH−ion bonds, which rupture the one-dimensional hydrogen bonding network found in pure glycerol.[24,52] This network is responsible for shuttling D^+/H^+ away from Cl^- after DCl ionizes in the interfacial region,[51,53] leading to bulk solvation of Cl^- and H^+ as the dominant reaction channel. In the presence of ions, this disruption of the Grotthuss proton relay should impede H^+ transport and thereby promote recombination of Cl^- with D → H-exchanged H^+, followed by HCl desorption before the ions separate again.

The large and hydrophobic THA^+ ion is unlikely to reorient interfacial OH groups sufficiently to break the connectivity of the glycerol hydrogen bonds. As illustrated in Figure 1 and in separate studies, water molecules surrounding tetrabutylammonium ions and ion pairs form a hydrogen bonding network that is at least as strong and as numerous as those in pure water.[3,4,16,43,54] In the case of THABr−glycerol solutions, surface glycerol molecules may align their CH_2CHCH_2 backbone against the hexyl chains, allowing OH groups along the backbone to participate in hydrogen bonding and aid in the transport of H^+ away from Cl^-. In accord with this picture, the enhancement in interfacial proton exchange by THABr (2.7% → 4.7%) is less than half that of NaBr (2.7% → 7.7%). This comparison suggests that both Na^+ and Br^- ions catalyze rapid D → H exchange in the NaBr solution, whereas only Br^- promotes this exchange in the THABr solution.

THA^+ ions may also interfere directly with OH−Br^- bonding at the high concentration of ions in the surface region, most likely as Br^- intermixes with the hexyl chains[54,55] or as glycerol restructuring around THA^+ reduces the number of OH groups that can bond to neighboring Br^- ions. An analogous reduction in the hydration of Na^+ has been observed in simulations of a mixture of NaCl and tetramethylammonium chloride in water.[56] These interactions would tend to isolate the Br^- ions, perhaps contributing to the smaller enhancement in interfacial proton exchange by THABr than by NaBr.

Concluding Remarks: Ionic Surfactants versus Ionic Solutions

The comparisons in Figure 9 between an ionic surfactant and alkali halide salt underscore the ability of solvated ions to promote rapid D → H exchange and reduce DCl entry. Although the 0.03 M THABr solution is 90 times less concentrated than the 2.7 M NaBr solution, the interfacial ion concentrations are similar (∼8×10^{13} cm^{-2} for THA^+ and Br^- versus ∼7×10^{13} cm^{-2} for Na^+ and Br^-). Interfacial THA^+ ions should be located primarily in the top solvent layer, with a deficit of THA^+ just below.[10] The Br^- counterions are likely to be located in the top or nearby layers, as found experimentally for tetrabutylammonium and tetrabutylphosphonium bromide in formamide,[7,30] and perhaps pulled even closer to the surface by THA^+ than in the NaBr−glycerol solution.[15] The segregation of Br^- and THA^+ implies that ions in the surface region, and not those in the bulk, are responsible for the 2-fold changes in DCl desorption and D → H exchange in Figure 9.

These observations support our earlier pulsed-beam experiments.[21,24] The location of rapid D → H exchange was previously inferred for pure glycerol and the alkali halide solutions via the prechopper measurements in Figure 8. These experiments place an upper limit on the bulk-phase solvation time for DCl/Cl^-/HCl species of 10^{-6} s, which corresponds to a diffusion depth of 10 Å. The use of surfactant ions provides an independent verification of this proximity to the surface, because it does not depend on timing experiments or diffusion models.

The propensity for both THABr and NaBr solutions to catalyze interfacial DCl−glycerol reactions highlights the key role of "frontier" ions, regardless of whether these ions are brought to the surface because they are surfactants or accompany them, or because their bulk concentration is high. In this sense, ion-mediated DCl desorption and D → H exchange are local processes that do not require ion participation many Angstroms deep into the solution. Figure 9 shows that this catalysis proceeds even if the cation is hydrophobic and does not bond strongly to the solvent. We hope to extend this comparison by substituting the weakly coordinating ClO_4^- anion[57,58] for Br^- in order to test the potentially unique role of halide ions in altering the surface reactivity of protic liquids.

Appendix: Residence Times of HCl in Pure and THABr−Glycerol

The exposure of glycerol to HCl gas generates H^+ and Cl^- ions in solution. An increasing fraction of these ions recombine and desorb as the exposure time increases, and the desorption flux rises with time until it asymptotically matches the flux of molecules entering solution and equilibrium is established. As shown in refs 20 and 23, a characteristic residence time for the ions in solution may be defined by

$$\tau = D\left(\frac{4K_{HCl}RT}{{\beta_{th}}^2 \nu_{th} {f_{HCl}^{\pm *}}^2 F_{beam}}\right)\left(\frac{N_A}{1000}\right) \qquad (A.1)$$

This equation was written incorrectly in refs 20 and 23. In this expression, D is the joint diffusion coefficient for H^+ and Cl^-, $f_{HCl}^{\pm *}$ is the mean molar activity coefficient of H^+ and Cl^- in a saturated solution, β_{th} is the HCl entry probability under thermal collision conditions with an average velocity ν_{th}, F_{beam} is the flux of HCl molecules on the surface, and $K_{HCl} = (f_{HCl}^{\pm *2}[H^+*][Cl^-*])/P_{HCl}$ is the equilibrium constant for HCl (g) ⇌ H^+ (gly) + Cl^- (gly). τ is equal to the time for the instantaneous desorption flux to rise to ∼49% of the entering flux. The dependence of τ on β_{th} may be understood from two constraints at equilibrium: the fluxes of HCl into and out of the liquid are equal and the H^+ and Cl^- concentrations are fixed for a given HCl gas concentration. To maintain these conditions, a lower HCl entry probability (lower entering flux) must be accompanied by a lower HCl exit probability (lower exiting flux) and, therefore, a longer H^+ and Cl^- residence time in the liquid at a constant H^+ and Cl^- concentration.

For pure glycerol and 0.03 M THABr−glycerol, the ratio of residence times is

$$\frac{\tau_{\mathrm{THABr}}}{\tau_{\mathrm{pure}}} = \left(\frac{\beta_{\mathrm{th}}^{\mathrm{pure}}}{\beta_{\mathrm{th}}^{\mathrm{THABr}}} \frac{f_{\mathrm{HCl,\ pure}}^{\pm *}}{f_{\mathrm{HCl,\ THABr}}^{\pm *}} \right)^2 \qquad \text{(A.2)}$$

assuming that the diffusion coefficients are the same in the two solutions. The entry probability, β_{th}, is given by $p_{\mathrm{solv}}/p_{\mathrm{trap}}$ in Figure 9. The activity coefficients are estimated using the extended Debye−Hückel approximation

$$\log(f^{\pm *}) = \frac{A\sqrt{M}}{1 + Bd\sqrt{M}} \qquad \text{(A.3)}$$

where $A = 1.40\ \mathrm{M}^{-1/2}$ and $B = 0.46\ \mathrm{M}^{-1/2}\ \text{Å}^{-1}$ for glycerol at 292 K, and d is chosen to be 5.6 Å, which is the distance of closest approach in water.[59,60] The impinging HCl flux is estimated from Figure 10 in ref 20 to be $\sim 8 \times 10^{14}\ \mathrm{cm}^{-2}\ \mathrm{s}^{-1}$, which generates a saturation concentration of HCl of 1 mM and $f_{\mathrm{HCl,\ pure}}^{\pm *}$ of 0.91. Equation A.3 also predicts that that $f_{\mathrm{HCl,\ THABr}}^{\pm *}$ is 0.67 for the 0.031 M THABr solution. This lower activity coefficient reflects the greater stabilization of H^+ and Cl^- by THA^+ and Br^-, and lengthens the time HCl spends in the solution before desorbing.

The estimated activity coefficients, along with the $p_{\mathrm{solv}}/p_{\mathrm{trap}}$ values of 0.87 for pure glycerol and 0.75 for THABr, yield $\tau_{\mathrm{THABr}}/\tau_{\mathrm{pure}} = 2.5$, which is 11% lower than the experimentally determined ratio of 2.8 ± 0.7 from $\tau = 0.40 \pm 0.05$ s in pure glycerol and 1.1 ± 0.3 s in 0.03 M THABr. The predicted ratio would be larger if the higher viscosity of the THABr solution was taken into account.[1] This good agreement demonstrates that even the addition of small amounts of salt can significantly increase the residence times of Cl^- and H^+ in glycerol.

Acknowledgment. We are grateful to the National Science Foundation for funding this research. We also thank Luboš Vrbka and Pavel Jungwirth for helpful discussions and for providing Figure 1.

References and Notes

(1) Wen, W.-Y. Aqueous Solutions of Symmetrical Tetraalkylammonium Salts. In *Water and Aqueous Solutions: Structure, Thermodynamics, and Transport Processes*; Horne, R. A., Ed.; Wiley-Interscience: New York, 1972; p 613.
(2) Marcus, Y. *J. Solution Chem.* **2008**, *37*, 1071.
(3) Slusher, J. T.; Cummings, P. T. *J. Phys. Chem. B* **1997**, *101*, 3818.
(4) Stangret, J.; Gampe, T. *J. Phys. Chem. B* **1999**, *103*, 3778.
(5) Tamaki, K. *Bull. Chem. Soc. Jpn.* **1974**, *47*, 2764.
(6) Andersson, G.; Morgner, H.; Schulze, K. D. *Nucl. Instrum. Methods B* **2002**, *190*, 222.
(7) Andersson, G.; Krebs, T.; Morgner, H. *Phys. Chem. Chem. Phys.* **2005**, *7*, 2948.
(8) Ballard, R. E.; Jones, J.; Sutherland, E. *Chem. Phys. Lett.* **1984**, *112*, 310.
(9) Holmberg, S.; Yuan, Z. C.; Moberg, R.; Siegbahn, H. *J. Electron Spectrosc.* **1988**, *47*, 27.
(10) Eschen, F.; Heyerhoff, M.; Morgner, H.; Vogt, J. *J. Phys.: Condens. Matter* **1995**, *7*, 1961.
(11) Winter, B.; Weber, R.; Schmidt, P. M.; Hertel, I. V.; Faubel, M.; Vrbka, L.; Jungwirth, P. *J. Phys. Chem. B* **2004**, *108*, 14558.
(12) Winter, B.; Weber, R.; Hertel, I. V.; Faubel, M.; Vrbka, L.; Jungwirth, P. *Chem. Phys. Lett.* **2005**, *410*, 222.
(13) Bergersen, H.; Marinho, R. R. T.; Pokapanich, W.; Lindblad, A.; Björneholm, O.; Sæthre, L. J.; Öhrwall, G. *J. Phys.: Condens. Matter* **2007**, *19*, 326101.
(14) Hrobárik, T.; Vrbka, L.; Jungwirth, P. *Biophys. Chem.* **2006**, *124*, 238.
(15) Jungwirth, P.; Tobias, D. J. *Chem. Rev.* **2006**, *106*, 1259.
(16) García-Tarrés, L.; Guàrdia, E. *J. Phys. Chem. B* **1998**, *102*, 7448.
(17) Vrbka, L.; Jungwirth, P. *Aust. J. Chem.* **2004**, *57*, 1211.
(18) Andersson, G.; Morgner, H. *Surf. Sci.* **2000**, *445*, 89.
(19) Newman, A. A. *Glycerol*; C. R. C. Press: Cleveland, 1968.
(20) Ringeisen, B. R.; Muenter, A. H.; Nathanson, G. M. *J. Phys. Chem. B* **2002**, *106*, 4988.
(21) Ringeisen, B. R.; Muenter, A. H.; Nathanson, G. M. *J. Phys. Chem. B* **2002**, *106*, 4999.
(22) Chorny, I.; Benjamin, I.; Nathanson, G. M. *J. Phys. Chem. B* **2004**, *108*, 995.
(23) Muenter, A. H.; DeZwaan, J. L.; Nathanson, G. M. *J. Phys. Chem. B* **2006**, *110*, 4881.
(24) Muenter, A. H.; DeZwaan, J. L.; Nathanson, G. M. *J. Phys. Chem. C* **2007**, *111*, 15043.
(25) DeZwaan, J. L.; Brastad, S. M.; Nathanson, G. M. *J. Phys. Chem. C* **2008**, *112*, 3008.
(26) THAI was not a feasible choice for these experiments because of its low solubility (which is only 5×10^{-4} molal in water). See ref 27.
(27) Nakayama, H.; Kuwata, H.; Yamamoto, N.; Akagi, Y.; Matsui, H. *Bull. Chem. Soc. Jpn.* **1989**, *62*, 985.
(28) Defay, R.; Prigogine, I. *Surface Tension and Adsorption*; Wiley: New York, 1966; Chapter 2.
(29) The glycerol value rises to $10 \times 10^{13}\ \mathrm{cm}^{-2}$ when activity coefficients for TBABr in acetonitrile are used in eq 1. This solvent was chosen because its dielectric constant of 38 is similar to the value of 41 for glycerol. See Barthel, J.; Kunz, W. *J. Solution Chem.* 1988, *17*, 399.
(30) Andersson, G.; Krebs, T.; Morgner, H. *Phys. Chem. Chem. Phys.* **2005**, *7*, 136.
(31) Butler, J. A. V.; Wightman, A. *J. Chem. Soc.* **1932**, *2089*.
(32) The effective van der Waals radius of THA^+ is estimated in ref 2 to be 4.7 Å. This yields a cross-sectional area $A_{\mathrm{THA+}} = \pi r_{\mathrm{vdw}}^2 = 70\ \text{Å}^2$ and predicts the smallest area for THA^+ among the different estimates reviewed in ref 2 (including partial molar volume in water). This 70 Å^2 estimate is corroborated by CPK molecular models, which indicate that each hexyl chain is roughly the size of a glycerol molecule. The area for Br^- is obtained from $r_{\mathrm{Br}^-} = 1.8$ Å (Cotton, F. A.; Wilkinson, G.; Murillo, C. A.; Bochmann, M. *Advanced Inorganic Chemistry*, 6th ed.; Wiley:New York, 1999; Appendix 4), and the average area of a glycerol molecule is calculated from its liquid phase density, $\rho = 1.26\ \mathrm{g\ cm}^{-3}$, and molecular weight, W, to be $A_{\mathrm{gly}} = (W/\rho)^{2/3}$.
(33) The surface excess Γ for the 2.7 M NaBr solution is $-9 \times 10^{13}\ \mathrm{cm}^{-2}$, assuming unit activity coefficients. This deficit drops to $-3 \times 10^{13}\ \mathrm{cm}^{-2}$ using activity coefficients measured for NaI in glycerol (ref 23). Even this deficit is likely to be too high because activity coefficients for NaBr in water are smaller than for NaI (ref 59).
(34) Lawrence, J. R.; Glass, S. V.; Nathanson, G. M. *J. Phys. Chem. A* **2005**, *109*, 7449.
(35) Glass, S. V.; Park, S.-C.; Nathanson, G. M. *J. Phys. Chem. A* **2006**, *110*, 7593.
(36) Köhler, S. P. K.; Reed, S. K.; Westacott, R. E.; McKendrick, K. G. *J. Phys. Chem. B* **2006**, *110*, 11717.
(37) Immediate HCl desorption is based on the small Henry's law constant for molecular HCl in hexadecane ($H \approx 0.2\ \mathrm{M\ atm}^{-1}$), which implies an average residence time shorter than the time for diffusion across a single glycerol layer. See eq 2 of ref 20.
(38) The HCl beam energy is 10 kJ mol^{-1} higher than the 90 kJ mol^{-1} DCl beam energy, leading to slightly smaller trapping and solvation probabilities for HCl than would have been measured for DCl. The measured value for pure glycerol of $p_{\mathrm{solv}} = 0.43 \pm 0.05$ is coincidentally identical to the average of 23 prior measurements for pure glycerol using 90 kJ mol^{-1} DCl. This coincidence reflects the small changes in trapping probability with incident energy and the uncertainty in the measurement (see Figure 8 of ref 20). We therefore did not rescale the p_{solv} values in Figure 6 but assumed that they may also be used for the present DCl experiments.
(39) See also Zolot, A. M.; Dagdigian, P. J.; Nesbitt, D. J. *J. Chem. Phys.* **2008**, *129*, 194705, which reports longtime evaporation (>1 ms) of HF from squalane following collisions of F atoms. This signal is attributed to emission of hot HF molecules from the liquid that strike the chamber walls, thermalize, and return to the probe region. In our experiments, the analogous source of HCl would be the 6% HCl impurity in the impinging DCl beam. The HCl signal arising from this impurity is subtracted from each TOF spectrum in Figures 7 and 8 by recording the HCl TOF spectrum generated by an impinging HCl beam created in the same way as the DCl beam. This subtraction procedure automatically removes from the TOF spectra the signal from any HCl molecules that strike the chamber walls and return to the probe region.
(40) $D \approx 5 \times 10^{-7}\ \mathrm{cm}^2\ \mathrm{s}^{-1}$ for HCl in squalane is estimated from the joint Cl^-/H^+ diffusion constant in water, $1.6 \times 10^{-5}\ \mathrm{cm}^2\ \mathrm{s}^{-1}$, times the ratio of viscosities, (1 cP/35 cP).
(41) The NaBr reaction probabilities measured in ref 24 are determined by scaling the HCl and DCl TOF signals from NaBr−glycerol to the values for pure glycerol recorded at the same time. The ratios are then multiplied by the average reaction probabilities for pure glycerol, as described in the Appendix of ref 24. The averages used in ref 24 were based on 11 measurements for pure glycerol. We have updated the reaction probabilities on the basis of a new average of 23 pure glycerol measurements. The

updated values for pure glycerol and NaBr−glycerol reported in Figure 9 lie within 10% of the values reported in ref 24.

(42) Wen, W.-Y. *J. Solution Chem.* **1973**, *2*, 253.

(43) Turner, J.; Soper, A. K. *J. Chem. Phys.* **1994**, *101*, 6116.

(44) Heinz, H.; Suter, U. W. *J. Phys. Chem. B* **2004**, *108*, 18341.

(45) Raugei, S.; Klein, M. L. *J. Chem. Phys.* **2002**, *116*, 196.

(46) Faralli, C.; Pagliai, M.; Cardini, G.; Schettino, V. *J. Phys. Chem. B* **2006**, *110*, 14923.

(47) Ayala, R.; Martínez, J. M.; Pappalardo, R. R.; Saint-Martin, H.; Ortega-Blake, I.; Marcos, E. S. *J. Chem. Phys.* **2002**, 10512.

(48) Carrillo-Tripp, M.; Saint-Martin, H.; Ortega-Blake, I. *J. Chem. Phys.* **2003**, *118*, 7062.

(49) Ikeda, T.; Boero, M.; Terakura, K. *J. Chem. Phys.* **2007**, *126*, 034501.

(50) Bakker, H. J. *Chem. Rev.* **2008**, *108*, 1456.

(51) Zhuang, W.; Dellago, C. *J. Phys. Chem. B* **2004**, *108*, 19647.

(52) For the effect of ions on proton transport in aqueous solutions, see Hertz, H. G.; Versmold, H.; Yoon, C. *Ber. Bunsenges. Phys. Chem.* **1983**, *87*, 577. Diratsaoglu, J.; Hauber, S.; Hertz, H. G.; Müller, K. J. *Z. Phys. Chem.* **1990**, *168*, 13. Choe, Y.-K.; Tsuchida, E.; Ikeshoji, T. *J. Chem. Phys.* **2007**, *126*, 154510.

(53) Morrone, J. A.; Tuckerman, M. E. *J. Chem. Phys.* **2002**, *117*, 4403.

(54) Buchner, R.; Hölzl, C.; Stauber, J.; Barthel, J. *Phys. Chem. Chem. Phys.* **2002**, *4*, 2169.

(55) Kunz, W.; Turq, P.; Calmettes, P.; Barthel, J.; Klein, L. *J. Phys. Chem.* **1006**, *96*, 2743.

(56) Kuba, A.; Hawlicka, E. *J. Mol. Liq.* **2004**, *112*, 91.

(57) Heinje, G.; Luck, W. A. P.; Heinzinger, K. *J. Phys. Chem.* **1987**, *91*, 331.

(58) Moberg, R.; Bokman, F.; Bohman, O.; Siegbahn, H. *J. Am. Chem. Soc.* **1990**, *113*, 3663.

(59) Robinson, R. A.; Stokes, R. H. *Electrolyte Solutions*, 2nd ed.; Academic Press: New York, 1959.

(60) Harned, H. S.; Owen, B. B. *The Physical Chemistry of Electrolyte Solutions*; Reinhold: New York, 1958; Chapter 12.

JP900232V